ARTICLE

JOURNAL OF Applied Polymer SCIENCE WILEY

Structurally modified poly(methyl methacrylate) electrospun nanofibers as better host matrix for noble metal nanoparticles

Princy Philip[1] | **Tomlal Jose**[1] | **Manoj Parameswaran**[2] | **Sajini Thankaraj**[1]

[1]Research and Postgraduate Department of Chemistry, St. Berchmans College, Mahatma Gandhi University, Kottayam, India

[2]Department of Chemistry, St. Michaels College, Kerala University, Alappuzha, India

Correspondence
Tomlal Jose, Research and Postgraduate Department of Chemistry, St. Berchmans College, Mahatma Gandhi University, Kottayam, Kerala 686101, India.
Email: tomlalj27@gmail.com

Abstract

Poly(methyl methacrylate) (PMMA) nanofibers are proved as good host matrix for various nanomaterials. Here, the possibilities offered by the process of electrospinning are exploited for the production of pure and structurally modified surface roughened and coaxial hollow PMMA electrospun nanofibers with unique advantages and surface characteristics, which is proved through various structural analyses. The host matrix nature of these pure and structurally modified surface roughened and coaxial hollow PMMA nanofibers to gold nanoparticles (AuNPs) are proved through different structural and morphological analyses. The host matrix nature of pure and structurally modified surface roughened and coaxial hollow PMMA nanofibers to AuNPs are compared with that of pure PMMA nanofibers by comparing their structural and optical properties. It is found here that, the surface roughened PMMA nanofibers act as better host matrix with more uniform distribution of particles and intensity enhancement than the pure and coaxial hollow PMMA nanofibers. Pure and coaxial hollow PMMA nanofibers show almost two times enhancement in intensity while the surface roughened PMMA nanofibers show almost five times enhancement in intensity after incorporating AuNPs. The host matrix nature of PMMA nanofibers is thus proved to be improved by making structural modifications on PMMA nanofibers in a simple and cost-effective way. This makes them more suitable and adaptable in their applications. This superior property of surface roughened PMMA nanofibers over pure PMMA nanofibers can be used in all the application fields of PMMA nanofibers like optical works, catalytically supporting agents, antibacterial supporting systems and so on.

KEYWORDS
host matrix, noble metal nanoparticles, photoluminescence, PMMA, surface modifications

1 | INTRODUCTION

Nanoscience and nanotechnology are ever-developing areas in the world, which unveils the mysteries of science to the mankind day by day. It is an on-going process and research, which nourishes and enriches the human life in all its aspects and senses. Various nanomaterials like nanoparticles, nanotubes, nanowires, nanofibers,

quantum dots, fullerenes are playing their own roles in the materials science world according to their unique properties and characteristics. For example, nanofibers are used in water purification systems, biomedical areas and so on,[1–4] nanoparticles for anticancer treatments and catalytic activities,[5] quantum dots for photocatalytic applications and degradation studies,[6,7] nanotubes for sensors[8] and so on. Nanofibers are considered as the smart materials of future out of their unique properties that make them suitable to the present requirements that the world demands. The polymer nanofibers can be synthesized by a variety of methods like drawing, template synthesis, phase separation, self-assembly, and electrospinning.[1] All the above-mentioned methods have their own characteristics and applications where electrospinning is also not an exception, as the electrospun nanofibers are compatible to the growing needs and situations of materials sciences and polymer community.

Electrospinning is the recent and most feasible method applied for the production of polymer nanofibers in massive and continuous form[2] as the electrospun polymer nanofibers have several advantages over the other way produced nanofibers. Some of them are their high surface area to volume ratio, tuneable porosity, malleability to conform to a wide variety of sizes and shapes, continuous production of polymer nanofibers in the submicron range, possibility of structural and surface modifications, feasible at room temperature, easiness of production and so on.[2,3,9] Recent studies reveal the design of a self-powered electrospinning system, which will further enhance the feasibility of electrospinning.[10,11] Electrospun polymer nanofibers find a wide variety of applications in various areas like tissue engineering, biomedical, water purification, energy conservation, environmental safety, catalytic processes, electronics, solar cells etc., as evidenced in the referred literatures.[12–23]

Poly(methyl methacrylate) (PMMA) is a synthetic polymer available in the market with an affordable cost. It is characterized with ability to produce uniform nanofibers, good mechanical and optical properties, easiness to handle, good processing ability, higher environmental stability, resistance to molds and enzymes etc., which make it attractive to carry out our studies.[24,25] PMMA is one of the main polymers in making electrospun polymer blend nanofibers with polymers like polyaniline, polystyrene etc., as evidenced in literature.[26–31] The host matrix nature of PMMA nanofibers to various nanomaterials has already proven in our own previous studies[32] and is available in literatures.[4,33] Noble metal nanoparticles like gold nanoparticles are also a matter of study in the research world out of their applications in various fields like sensors,[34,35] protein determination,[36] catalytic reductions,[37,38] medical treatments[13] etc. AuNPs are characterized with many advantages also, where high surface area to volume ratio,[37] optical properties,[35] stability, nonpoisonous nature[39] etc. are a few among them.

Here, the novelty and difference from the other reported works lies in many facts. The host matrix nature of PMMA nanofibers, films etc., are already proved,[35,40,41] but the present work analyses and reports the host matrix nature of structurally modified PMMA nanofibers like surface roughened and coaxial hollow PMMA nanofibers over the pristine PMMA nanofibers for nanomaterials like gold nanoparticles (AuNPs) for the first time. Here, the structural modifications are made on PMMA nanofibers by preparing PMMA electrospun nanofibers in three ways: one in pure form; second, the surface roughened PMMA nanofibers by the selective dissolution of PEO from PEO—PMMA polymer blend electrospun nanofibers, and the third, coaxial hollow PMMA nanofibers by the selective removal of PEO from PEO—PMMA coaxial nanofibers. Surface roughened PMMA nanofibers are characterized with voids, pits etc. on the surface, and coaxial hollow PMMA nanofibers have a hollow space in the core, as evidenced in the coming sections, by the removal of PEO from PEO—PMMA polymer blend and coaxial nanofibers. These properties make them more advantageous as they can hold a greater number of particles as described in the following sections.

Herein our work has two main stages where first one deals with the preparation of pure, surface roughened and coaxial hollow PMMA nanofibers and the second one deals with the preparation and characterization of these pure and structurally modified PMMA nanofibers incorporated with AuNPs. Thus, the work tries to fill up the gap of surface modifications possible through electrospinning by tuning its various parameters, which is a major step in improving the properties and applications of polymer nanofibers. The present study also aims to narrate the ways to improve the host matrix nature of PMMA nanofibers to AuNPs by synthesizing surface roughened and coaxial hollow PMMA nanofibers in a simple, cost-effective and eco-friendly way, with full evidence by checking their host matrix nature to AuNPs.

2 | MATERIALS AND METHODS

2.1 | Materials

The various materials used in the study are poly(methyl methacrylate) (PMMA) (molecular weight 15,000 g mol^{-1}, Alfa Aesar), poly(ethylene oxide) (PEO) (Molecular Weight

FIGURE 1 Electrospinning machine [Color figure can be viewed at wileyonlinelibrary.com]

FIGURE 2 Experimental setup for the selective dissolution of PEO from PEO–PMMA polymer nanofibers [Color figure can be viewed at wileyonlinelibrary.com]

100,000 g mol^{-1}, Sigma Aldrich), chloroform (Merk) and acetone (Merk) and colloidal AuNPs.

2.2 | Methods

2.2.1 | Preparation of pure and structurally modified PMMA nanofibers

The pure and structurally modified forms like surface roughened and coaxial hollow PMMA nanofibers are produced by tuning the electrospinning parameters. Pure PMMA nanofibers are produced by dissolving approximately 1 g of PMMA in a binary mixture of acetone and chloroform, which is then subjected to electrospinning with 0.45 ml/hr flow rate, 20 kV voltage and 20 cm tip to collector distance. The surface roughened PMMA nanofibers are produced by the selective dissolution of PEO from PEO–PMMA polymer blend electrospun nanofibers. The PEO–PMMA polymer blend electrospun nanofibers, which are a very rare combination in the electrospinning world is produced with 10 kV applied voltage, 0.4 ml/hr flow rate and 16 cm tip to collector distance. The coaxial hollow PMMA nanofibers are also produced from coaxial PEO–PMMA nanofibers where PEO is the core and PMMA is the sheath. Here both the core PEO and sheath PMMA nanofibers are produced by applying 19 kV voltage, 20 cm tip to collector distance and 0.5 ml/hr flow rate in the electrospinning process. Coaxial hollow PMMA nanofibers are produced by the selective dissolution of PEO from the coaxial PEO–
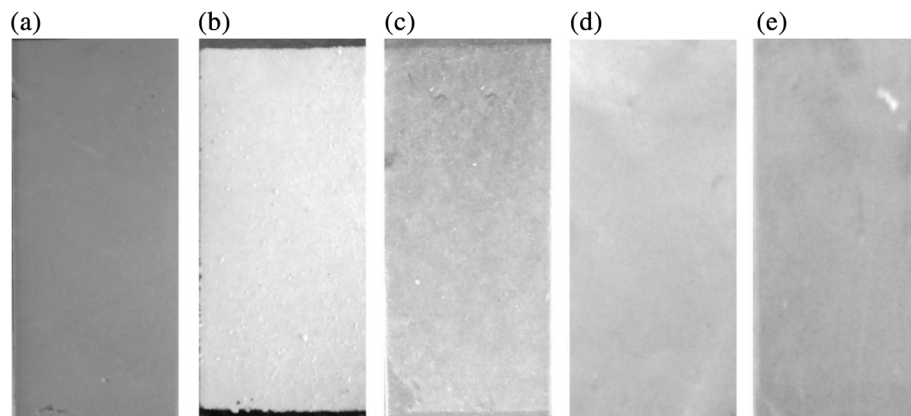
FIGURE 3 Photos: (a) pristine PMMA nanofibers (b) PEO–PMMA blend nanofibers (c) surface roughened PMMA nanofibers (d) coaxial PEO–PMMA nanofibers (e) coaxial hollow PMMA nanofibers

TABLE 1 Parameters of electrospinning

No:	Sample	Type of syringe (ml)	Applied voltage (kV)	Flow rate (ml/hr)	Distance (cm)
1	Pristine PMMA	10	20	0.5	20
2	PEO–PMMA blend	2	10	0.4	16
3	Coaxial PEO–PMMA	Core: 5; sheath: 10	19	0.5	20

PMMA nanofibers. Selective dissolution of PEO from PEO–PMMA nanofibers is carried out using deionized water at 60°C in both surface roughened and coaxial hollow nanofibers. The detailed procedure for the preparation of pure, surface roughened and coaxial hollow PMMA nanofibers and the analyses of each of them are given in our previously published papers.[32,42]

Figure 1 shows the electrospinning machine that we have used for the production of PMMA nanofiber and Figure 2 shows the experimental setup for the production of surface roughened and coaxial hollow PMMA nanofibers by selective dissolution of PEO from PEO–PMMA blend and coaxial nanofibers. The photos of the produced pure and structurally modified PMMA nanofibers are given in Figure 3. The various parameters applied for the production of pure and structurally modified PMMA nanofibers are summarized in Table 1.

2.2.2 | Preparation of pure and structurally modified PMMA nanofibers incorporated with AuNPs

The experimental setup for the production of pure and structurally modified PMMA nanofibers incorporated with AuNPs is shown in Figure 4. The pure, surface roughened and coaxial hollow PMMA nanofibers incorporated with AuNPs having 17.97 nm diameter are produced by dispersion method. 0.02 g of the pure, surface roughened and coaxial hollow PMMA nanofibers are immersed in 10 ml of colloidal AuNPs in separate small

petridishes for 3 weeks and then we get the AuNPs incorporated PMMA nanofibers. The experimental setup for the production of pure and structurally modified PMMA nanofibers incorporated with AuNPs is shown in Figure 4.

3 | MEASUREMENTS

FTIR analyses of the samples are carried out using Perkin Elmer Spectrum Two; XRD analyses of the samples are carried out with Rigaku MiniFlex 600 X-ray Diffractometer; EDX analyses of the samples are carried out using JEOL Model-JSM 6390LV; AFM analyses of the samples are carried out with Alpha300RA AFM & RAMAN; FESEM analyses of the samples are carried out with Nova NanoSEM 450 UoK; TEM analyses are conducted with High Resolution Transmission Electron Microscope Facility, JEM 2100; UV and PL analyses are carried out using FL3-211_1939C-5017-FL.

4 | RESULTS AND DISCUSSION

The pure, surface roughened and coaxial hollow electrospun PMMA nanofibers incorporated with gold nanoparticles are subjected to various characterization techniques to analyze the influence and impact of these gold nanoparticles on the structural and morphological properties of pure and structurally modified PMMA nanofibers.

FIGURE 4 Experimental setup for the incorporation of gold nanoparticles into PMMA nanofibers with different architectures [Color figure can be viewed at wileyonlinelibrary.com]

FIGURE 5 FTIR spectra: (a) pristine PMMA nanofibers (b) pristine PMMA nanofibers incorporated with AuNPs (c) surface roughened PMMA nanofibers (d) surface roughened PMMA nanofibers incorporated with AuNPs (e) coaxial hollow PMMA nanofibers (f) coaxial hollow PMMA nanofibers incorporated with AuNPs [Color figure can be viewed at wileyonlinelibrary.com]
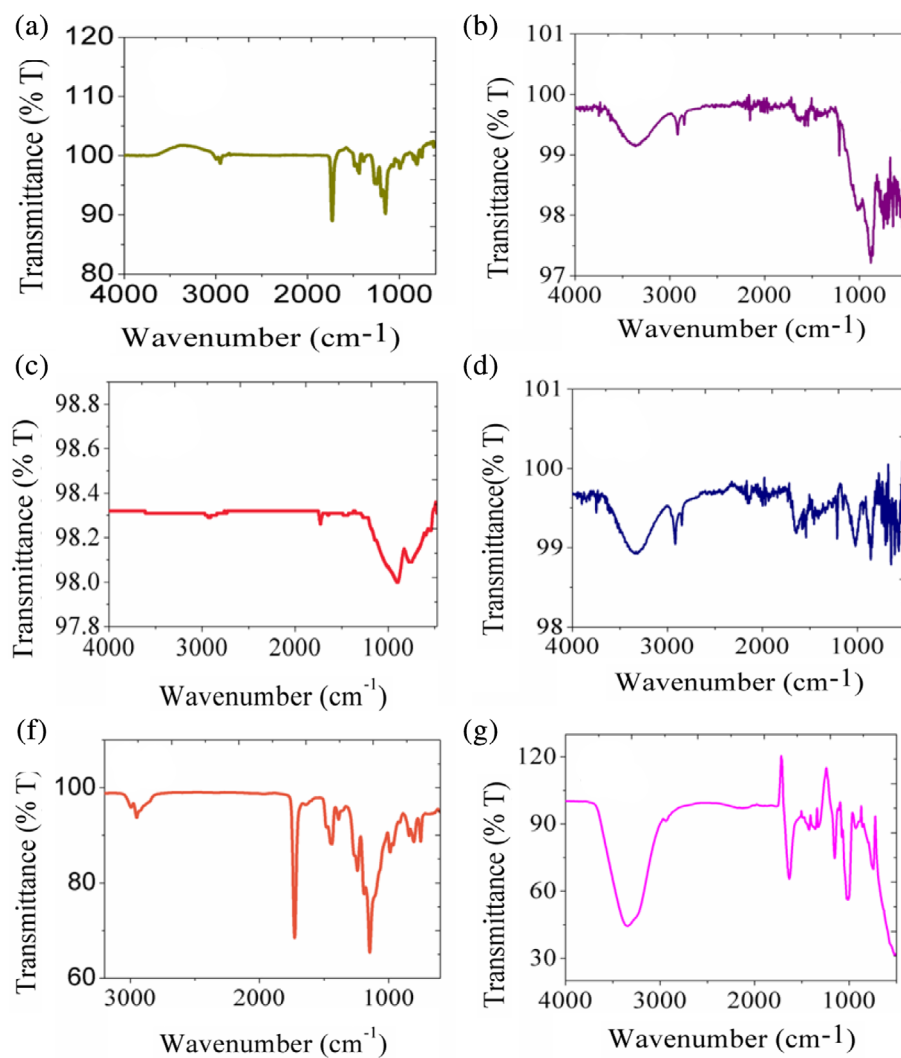
4.1 | Fourier transform infrared spectra (FTIR) analysis

FTIR spectra of the pristine, surface roughened and coaxial hollow PMMA electrospun nanofibers and that incorporated with gold nanoparticles are shown in Figure 5a–f. The FTIR peak assignments of pure, surface roughened and coaxial hollow PMMA nanofibers and those incorporated with gold nanoparticles are given in Tables 2 and 3, respectively. It is given that, pristine

TABLE 2 FTIR spectral assignments of the pristine, surface roughened and coaxial hollow PMMA electrospun nanofibers

Sample	Wavenumber (cm^{-1})	Assignment of peaks
Pristine PMMA nanofibers	2949	C—H stretching band
	1730	C=O band
	1435	H—C—H bend
	1149	C—O—C
	990	C—C stretching
	807	C=O in plane bending
Surface roughened PMMA nanofibers	2921	C—H stretching band
	1728	C=O band
	1405	H—C—H bend
	1145	C—O—C
	900	C—C stretching
	762	C=O in plane bending
Coaxial hollow PMMA nanofibers	2949	C—H stretching band
	1727	PMMA C=O band
	1435	H—C—H Bend PMMA
	1146	C—O—C Stretching Vibration
	988	C—C Stretching PMMA
	805	C=O in plane Bending

PMMA show peaks at 2949 and 1730 cm^{-1}, which indicates the C—H stretching band and C=O group in PMMA, respectively. PMMA peaks of H—C—H bend, C—O—C stretching, C—C stretching, C=O in plane bending and C=O out of plane bending are obtained at 1435, 1149, 990, 807, and 751 cm^{-1}, respectively.[42]

It is observed from the FTIR spectra of PMMA nanofibers incorporated with gold nanoparticles that certain new peaks are observed here and also the peaks of PMMA show a blue shift. The broad peak obtained at 3200–3600, 2918, 1623, 1370, 1215, and 1019 cm^{-1}, respectively, corresponds to the stretching vibrations of OH group, aliphatic C—H stretching vibrations, C=C stretching vibrations, OH bending vibrations, C—OH bending vibrations, C—O stretching vibrations of phenolic group and aromatic ring. The peak at 826 cm^{-1} is characteristic of the aromatic ring. These bands arise from the alkaloids and various phytochemicals present in the leaf extract from which the gold nanoparticles are made and all the details related to the preparation and characterization of AuNPs are given in literature.[43] Here it is observed that the FTIR peaks of PMMA shifted to 2955, 1739, 1456, 994, and 810 cm^{-1}, which denotes PMMA C—H stretching band, PMMA C=O band, H—C—H bend in PMMA, C—C stretching PMMA, C=O in plane bending, respectively.

Surface roughened PMMA nanofibers show peaks at 2921, 1728, 1145, 900, and 760 cm^{-1}, which, respectively, represents PMMA C—H stretching band, PMMA C=O band, C—O—C band, C—C stretching band and C=O in plane bending as mentioned.[42] Surface roughened PMMA nanofibers incorporated with AuNPs also show characteristic peaks of both PMMA and AuNPs. Here, the broad peaks at 3000–3700 cm^{-1} shows the stretching vibrations of OH group, 2918 cm^{-1} show aliphatic C—H stretching vibrations, 1644 cm^{-1} show C=C stretching vibrations, 1332 cm^{-1} show OH bending vibrations, 1217 cm^{-1} show OH bending vibrations, 1019 cm^{-1} show C—O stretching vibrations of phenolic group and aromatic ring. Here it is found that, the FTIR peaks of surface roughened PMMA nanofibers are shifted to 2958, 1733, 1149, 935 cm^{-1}, which represents PMMA C—H stretching band, PMMA C=O band, C—O—C stretching vibrations and C—C stretching, respectively.

Coaxial hollow PMMA nanofibers show peaks at 2949, 1727, 1435, 1146, 988, 805, and 751 cm^{-1}, which denotes C—H stretching band, C=O band, H—C—H bend, C—O—C stretching vibration, C—C stretching, C=O in plane bending and C=O out of plane bending respectively. Coaxial hollow PMMA nanofibers incorporated with gold nanoparticles show peaks at 3000–3700 cm^{-1}, which denotes the stretching vibrations of OH group, 1630 cm^{-1} show C=C stretching vibrations, 1325 cm^{-1} that points to OH bending vibrations, 1242 cm^{-1} corresponding to C—OH bending vibrations, 1013 cm^{-1} of C—O stretching vibrations of phenolic group and aromatic ring. Here, after incorporating AuNPs to coaxial hollow PMMA nanofibers the FTIR peaks of coaxial hollow PMMA nanofibers are shifted to 2947, 1717, 1410, 1142 cm^{-1} etc., which represents C—H stretching band, PMMA C=O band, H—C—H Bend PMMA, C—O—C stretching vibration, respectively.

The shift occurs in the FTIR peaks of PMMA nanofibers after incorporating AuNPs is due to the functional group interaction between PMMA and gold nanoparticles. A weak bond is formed between PMMA and AuNPs and the interaction between PMMA and AuNPs is referred here.[44] Thus, the FTIR spectra prove that PMMA can act as good host matrix to AuNPs.

4.2 | X-ray diffractometer (XRD) analysis

X-ray diffractometer (XRD) spectra of the pure, surface roughened, coaxial hollow PMMA nanofibers and those incorporated with gold nanoparticles are shown in Figure 6. It has already given that pure PMMA nanofibers show XRD peaks at 24.18°, 43.19°, and 63.1°[42] but here it is observed that they are shifted to 23.7°,

TABLE 3 FTIR spectral assignments of the pristine, surface roughened and coaxial hollow PMMA electrospun nanofibers incorporated with gold nanoparticles

Sample	Wavenumber (cm^{-1})	Assignments of peaks
Pristine PMMA nanofibers with gold nanoparticles	3200–3600	stretching vibrations of OH group
	2955	C—H stretching band
	2918	aliphatic C—H stretching vibrations
	1739	PMMA C=O band
	1623	C=C stretching vibrations
	1456	H—C—H bend in PMMA
	1215	OH bending vibrations
	994	C—C stretching PMMA
	826	C—O stretching vibrations
Surface roughened PMMA nanofibers with gold nanoparticles	3000–3700	stretching vibrations of OH group
	2958	C—H stretching band of PMMA
	2918	aliphatic C—H stretching vibrations
	1733	C=O band
	1644	C=C stretching vibrations
	1332	OH bending vibrations
	1217	OH bending vibrations
	1149	C—O—C stretching vibrations
	1019	C—O stretching vibrations of phenolic group
	935	C—C stretching
Coaxial hollow PMMA nanofibers with gold nanoparticles	3000–3700	stretching vibrations of OH group
	2947	C—H stretching band of PMMA
	1717	C=O band in PMMA
	1630	show C=C stretching vibrations
	1410	H—C—H Bend PMMA
	1325	OH bending vibrations
	1242	C—OH bending vibrations
	1142	C—O—C stretching vibration
	1013	C—O stretching vibrations

41.5°, and 62.5°, respectively after incorporating with gold nanoparticles. The shift in peaks is due to the interaction with AuNPs and that supports FTIR results. The peaks obtained at 38.2°, 44.5°, 64.8°, and 77.6° correspond to (1 1 1), (2 0 0), (2 2 0), and (3 1 1) reflections of FCC structured gold nanoparticles.[43] The sharp peak obtained at 38.2° is a clear indication of the presence of FCC structured gold nanoparticles.[38] Here, the XRD spectrum shows the characteristic peaks of both PMMA and gold nanoparticles that prove the incorporation of gold nanoparticles to PMMA polymer matrix.

Surface roughened PMMA nanofibers also possess characteristic peaks of PMMA at 29.28°, 44°, and 64.19° as mentioned in previous sections. The peaks are shifted to 22.8°, 43°, and 61.2°, respectively, after incorporating AuNPs to these nanofibers as shown in Figure 6d. Here, the peaks of AuNPs are very much suppressed by that of PMMA nanofiber peaks. It may be because of the fact that here in this case the AuNPs are present in the depressions, voids and pits of the surface roughened PMMA nanofibers rather than only on the surface as in the case of pure PMMA nanofibers.

Coaxial hollow PMMA nanofibers found to show peaks at 24.7°, 43.19° etc., as shown in Figure 6e while it is shifted to 25.8° and 46.8° after incorporating AuNPs to it. Here the peaks of AuNPs are found to be at 38.2°, 44.1°, 64.76°, and 77.7° but these peaks are suppressed and merged with PMMA peaks, which may be due to the
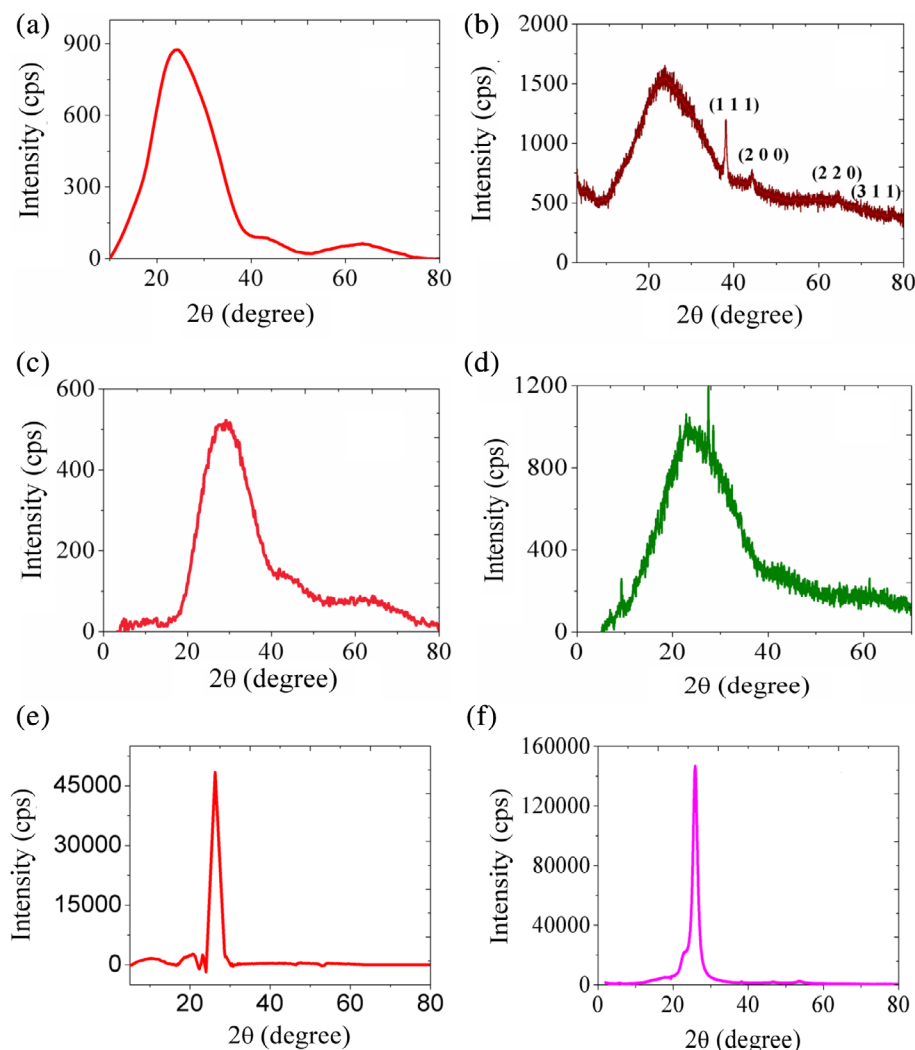
FIGURE 6 XRD spectra: (a) pure PMMA nanofibers (b) pure PMMA nanofibers incorporated with gold nanoparticles (c) surface roughened PMMA nanofibers (d) surface roughened PMMA nanofibers incorporated with gold nanoparticles (e) coaxial hollow PMMA nanofibers (f) coaxial hollow PMMA nanofibers incorporated with gold nanoparticles [Color figure can be viewed at wileyonlinelibrary.com]

substrate characteristic properties. The shift in PMMA peak position in all the fiber samples after incorporating AuNPs to the fiber samples clearly indicates the successful incorporation of AuNPs to PMMA nanofibers.

4.3 | Field emission scanning electron microscope (FESEM) analysis

Field emission scanning electron microscope (FESEM) analyses of the pure and surface roughened PMMA nanofibers are carried out to get an idea about the surface morphological changes in the PMMA nanofibers before and after incorporating AuNPs to it and the results are given in Figure 7a–d. FESEM images of the pure PMMA nanofibers and that incorporated with AuNPs show that the fibers are smooth with a clear surface while after incorporating AuNPs the clarity of the fiber surface disappears since AuNPs are attached to it as shown in Figure 7a,b, respectively. FESEM image of the surface roughened PMMA nanofiber shows the voids, pits,

depressions and so on. present on the fiber surface whereas that of the surface roughened PMMA nanofibers incorporated with AuNPs shows that they are covered by the AuNPs as shown in Figure 7c,d, respectively. Thus, the FESEM results support FTIR results.

The fiber diameter distribution diagrams of the samples are measured using WCIF Image J software and are given in Figure 8a–f. It is observed from the fiber diameter distribution diagrams that, pure PMMA nanofibers are found to be smooth and uniform with 60–150 nm diameters while after incorporating AuNPs the fibers are found to be nonuniform and diameter increases which proves the successful incorporation of the particles to PMMA host matrix. Surface roughened PMMA nanofibers have 80–120 nm diameters with uniform distribution of nanofibers while after incorporating AuNPs it increases upto 150 nm in nonuniform nature. Coaxial hollow PMMA nanofibers found to be in 100–150 nm diameters in their native form whereas it changes to 100–250 nm diameters after incorporating AuNPs to

FIGURE 7 FESEM images: (a) pure PMMA nanofibers (b) pure PMMA nanofibers incorporated with gold nanoparticles (c) surface roughened PMMA nanofibers (d) surface roughened PMMA nanofibers incorporated with gold nanoparticles
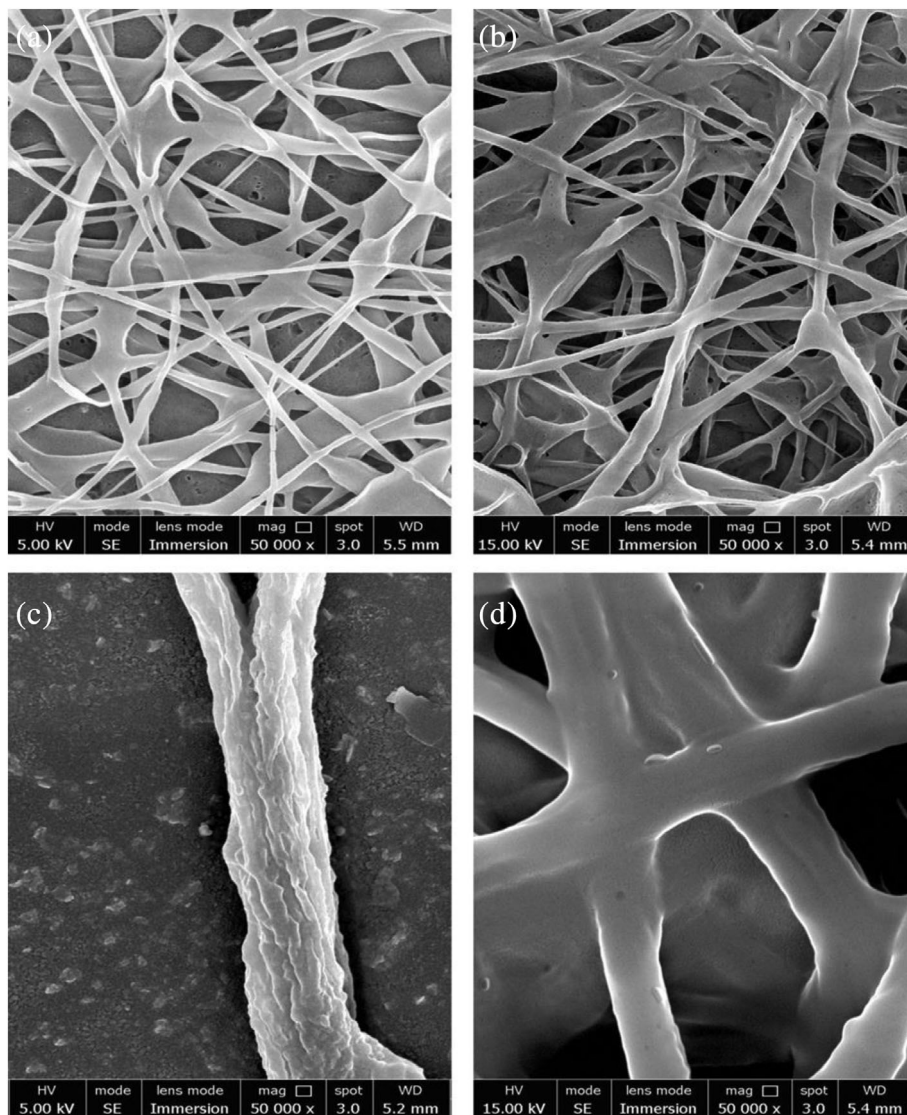
them. Here the fibers are found to be much more non-uniform than the other two forms of PMMA nanofibers.

The changes occurring in the diameters of the nanofibers, shape of the fiber diameter distribution diagrams and nonuniformity of fiber diameters in distribution diagrams after incorporating AuNPs gives a clear evidence for the successful incorporation of the AuNPs to these pure, surface roughened and coaxial hollow PMMA nanofibers. Thus, the host matrix character of PMMA nanofibers is clearly proved by FESEM analyses and the histograms.

4.4 | Transmission electron microscope (TEM) analysis

Transmission electron microscope (TEM) analyses of the samples are carried out to understand how the AuNPs are distributed in the pure and structurally modified

PMMA nanofibers and how the presence of crystalline AuNPs influences the amorphous properties of PMMA nanofibers. The TEM images of the coaxial hollow PMMA nanofibers that prepared by the selective removal of PEO from the coaxial PEO–PMMA is shown in Figure 9a and the detailed analyses of them are given in previously published paper.[42] The TEM images of the pure, surface roughened and coaxial hollow PMMA nanofibers after incorporating AuNPs are given in Figure 9b–d and the SAED pattern of each sample is shown in inset of the corresponding TEM images. Analyses of the TEM images show that surface roughened PMMA nanofiber show much more uniform distribution of AuNPs than the pure and coaxial hollow PMMA nanofibers. This is due to the surface characteristics of surface roughened PMMA nanofibers with many voids, pits etc., on all over the surface to occupy more AuNPs while such a property is absent in the other two forms. Coaxial hollow PMMA nanofibers contains large amount
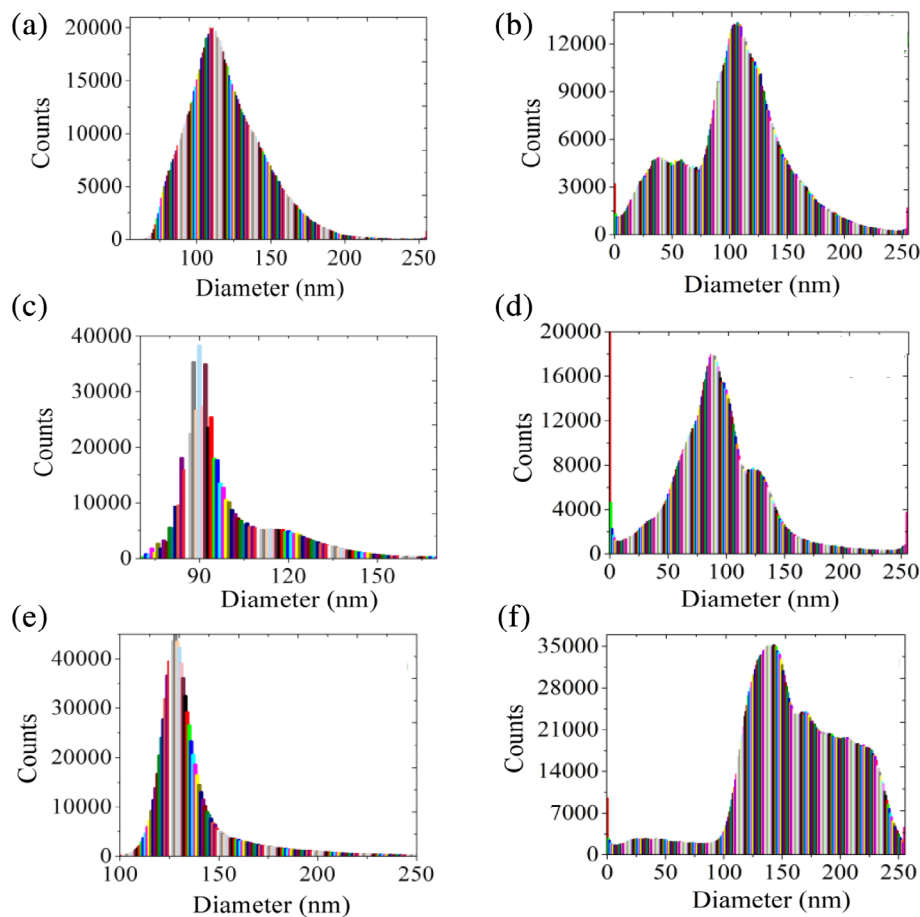
FIGURE 8 Fiber diameter distribution diagrams: (a) pure PMMA nanofibers (b) pure PMMA nanofibers incorporated with gold nanoparticles (c) surface roughened PMMA nanofibers (d) surface roughened PMMA nanofibers incorporated with gold nanoparticles (e) coaxial hollow PMMA nanofibers (f) coaxial hollow PMMA nanofibers incorporated with gold nanoparticles [Color figure can be viewed at wileyonlinelibrary.com]

of AuNPs but it is not distributed uniformly as shown in Figure 9c. So, it can be concluded here that surface roughened PMMA nanofibers with uniform distribution of particles are found to the better host matrix over pure and coaxial hollow PMMA nanofibers. The possibility to reduce the size of AuNPs after embedding in these PMMA nanofibers[45] is not significant here, as here the size of AuNPs are less than the fiber diameters that leads to the linear chain like arrangements of AuNPs.

4.5 | Energy dispersive X-ray spectroscopy (EDX) analysis

Energy dispersive X-ray spectroscopy (EDX) analyses of the samples are carried out to estimate the amount of AuNPs incorporated into the pure and structurally modified electrospun PMMA nanofibers.

EDX spectra of the pure, surface roughened and coaxial hollow PMMA samples incorporated with AuNPs are given in Figure 10a–c, respectively, and the elemental composition of the samples are given in Table 4, respectively. Pure PMMA nanofibers contain 0.42% of AuNPs while surface roughened PMMA nanofibers contain
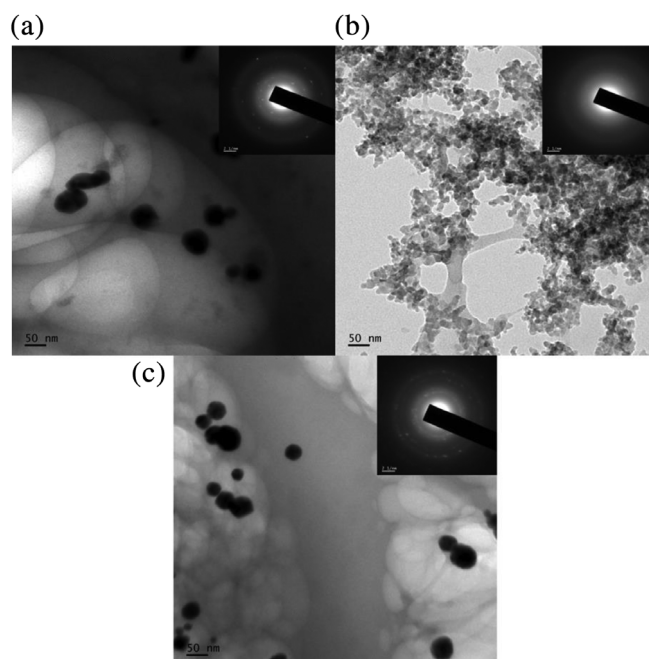

FIGURE 9 TEM images: (a) coaxial hollow PMMA nanofiber (inset: Coaxial PEO–PMMA nanofiber) (b) pure PMMA nanofibers incorporated with gold nanoparticles (c) surface roughened PMMA nanofibers incorporated with gold nanoparticles (d) coaxial hollow PMMA nanofibers incorporated with gold nanoparticles

2.58% and coaxial hollow PMMA nanofibers contain 40.07% of AuNPs. Here coaxial hollow PMMA nanofibers contain higher amount of AuNPs due to the presence of hollow space available in the coaxial hollow structures. Here the entry of AuNPs to this hollow space is possible since the colloidal AuNPs do not contain other bigger components from the source material, which prevent the entry of AuNPs to hollow space. But TEM analysis showed that surface roughened PMMA nanofibers show much more uniform distribution of the particles. EDX analysis measures the elemental composition at a particular point of the sample and hence the number of nanoparticles may not be uniform everywhere. The EDX spectra shows the linear chain like arrangement of AuNPs in the polymer nanofibers as evidenced in literature.[46] It can be concluded on comparing the TEM and EDX results that even though coaxial hollow PMMA nanofibers contain large amount of AuNPs surface roughened PMMA nanofibers are much more trustable since it possesses uniform distribution of AuNPs. Thus, the EDX analysis gives clear evidence for the incorporation of AuNPs to pure and structurally modified PMMA nanofibers. It also supports the TEM results.

4.6 | Atomic force electron microscope (AFM) analysis

The 3D atomic force electron microscope (AFM) images of the pure, surface roughened and coaxial hollow PMMA nanofibers and those incorporated with gold nanoparticles are shown in Figure 11a–f. The AFM images of the pure, surface roughened and coaxial hollow PMMA nanofibers incorporated with the gold nanoparticles are found to be entirely different from those of bare nanofibers, which evidence the successful incorporation of the nanoparticles to the fiber. Here the particles are found to be distributed wholly throughout the sample, which is an indication of the successful incorporation of the nanoparticles to the nanofibers. Here, the coaxial hollow PMMA nanofibers incorporated with AuNPs show some unique surface properties. It is observable from Figure 11b,d that the presence of AuNPs are clearly visible in the case of pure and surface roughened PMMA nanofibers incorporated with AuNPs; but, in the case of coaxial hollow PMMA nanofibers incorporated with AuNPs, it is not that much visible and it looks entirely different as shown in Figure 11f. This is because here the density of accumulation of particles is much higher than the other two types of PMMA nanofibers. This supports the TEM and EDX results. Thus, AFM analysis also works as an analytical tool to prove the incorporation of AuNPs to PMMA host matrix.
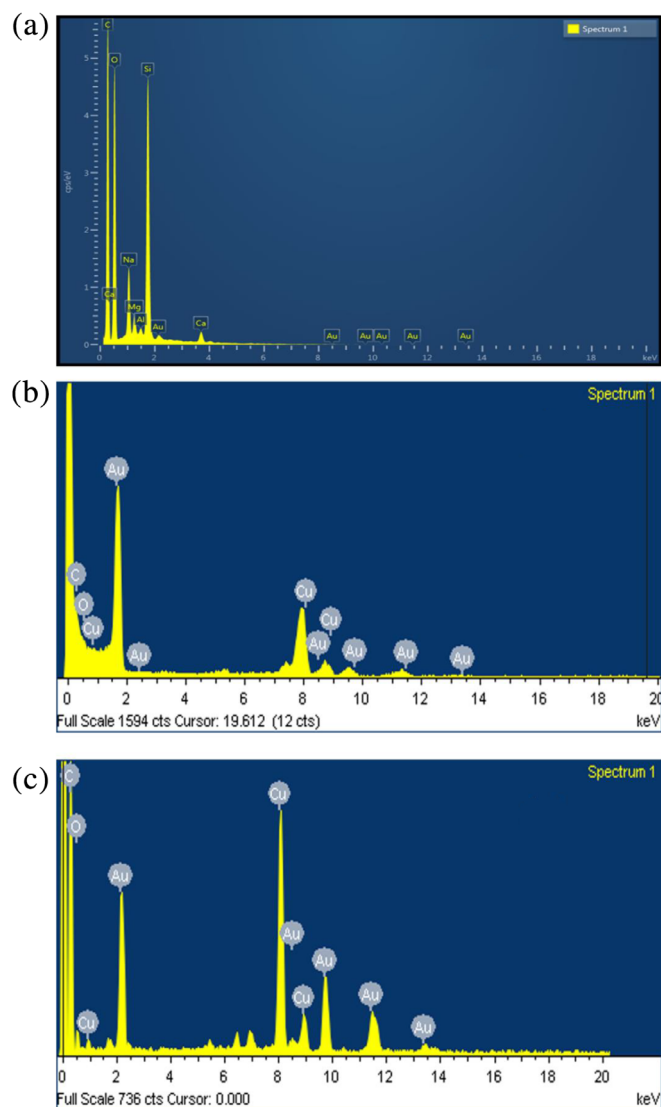

FIGURE 10 EDX spectra: (a) pure PMMA nanofibers incorporated with gold nanoparticles (b) surface roughened PMMA nanofibers incorporated with gold nanoparticles (c) coaxial hollow PMMA nanofibers incorporated with gold nanoparticles [Color figure can be viewed at wileyonlinelibrary.com]

4.7 | UV–Visible absorption (UV-Vis) analysis

The UV–Visible analysis spectra of pure, surface roughened, coaxial hollow PMMA nanofibers and these nanofibers incorporated with gold nanoparticles are shown in Figure 12a–f. All the pure and structurally modified PMMA nanofibers show a broad absorption in the visible region as mentioned in previously published paper[32] and the UV–Visible spectra of these nanofibers show a significant change after incorporating AuNPs to them. The broadness of the absorption band is reduced to a great extent after incorporating AuNPs to the fibers. The pure and surface roughened PMMA nanofibers do

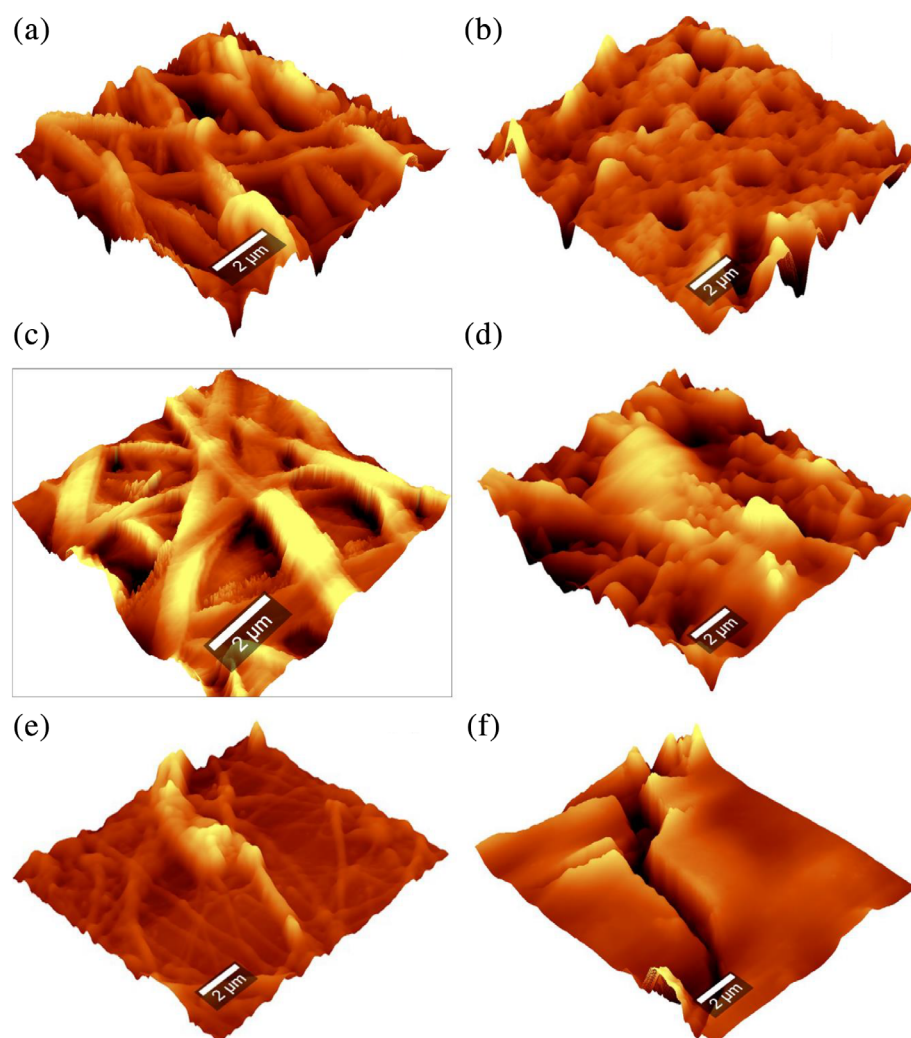| Sample	Element	Weight %	Atomic %
Pure PMMA nanofibers incorporated with AuNPs	C	49.81	59.54
	O	37.99	34.09
	Na	3.13	1.95
	Mg	0.64	0.38
	Al	0.18	0.1
	Si	7.29	3.73
	Ca	0.54	0.19
	Au	0.42	0.03
Surface roughened PMMA nanofibers incorporated with AuNPs	C	29.55	62.38
	O	8.60	13.63
	Cu	59.26	23.65
	Au	2.58	0.33
Coaxial hollow PMMA nanofibers incorporated with AuNPs	C	28.28	74.69
	O	2.05	4.07
	Cu	29.60	14.78
	Au	40.07	6.45

FIGURE 11 AFM images: (a) pure PMMA nanofibers (b) pure PMMA nanofibers incorporated with gold nanoparticles (c) surface roughened PMMA nanofibers (d) surface roughened PMMA nanofibers incorporated with gold nanoparticles (e) coaxial hollow PMMA nanofibers (f) coaxial hollow PMMA nanofibers incorporated with gold nanoparticles [Color figure can be viewed at wileyonlinelibrary.com]

not show separate peaks of AuNPs, which may be because of the shifting of the peaks of AuNPs to lower wavelengths and merging with that of PMMA. The absorption peaks of AuNPs are seen in coaxial hollow forms since the AuNPs are present in the hollow space inside the fiber.

Pure PMMA nanofibers with AuNPs show maximum absorption at 292 nm, surface roughened PMMA nanofibers with AuNPs have maximum absorption at 300 nm and the coaxial hollow PMMA nanofibers possess maximum absorption at 305 nm, which is entirely different from the absorption maxima of these fibers in their virgin form. Thus, the UV–Visible absorption analysis gives a solid support for the host matrix nature of PMMA nanofibers to AuNPs.

4.8 | Photoluminescence (PL) studies

The photoluminescence spectra of the pure PMMA nanofibers, surface roughened PMMA nanofibers, coaxial hollow PMMA nanofibers and those incorporated with gold nanoparticles are given in Figure 13a–f. Pure PMMA nanofibers are subjected to different excitation wavelengths and they show maximum emission at 330 nm as shown in Figure 13a. Pure PMMA nanofibers incorporated with AuNPs are subjected to excitation wavelengths ranging from 270 to 310 nm as shown in Figure 13b and it is observed that PMMA shows a broad emission in 400–500 nm range. The peaks of AuNPs are present at 530–550 nm[43] but here it is not that much visible since the concentration of AuNPs is very low as evidenced by EDX analysis. The peak obtained at 650–700 nm corresponds to the plant extract contents from which the AuNPs were made.[43] The intensity of the PL peaks found to increase with increase in excitation wavelength and it show maximum intensity at 310 nm with almost 600,000 cps where pure PMMA nanofibers show around 500,000 cps. The intensity of the PMMA nanofibers increases after incorporation of AuNPs since the luminescence nature and Surface Plasmon Resonance (SPR) of AuNPs adds to the transparency of PMMA nanofibers.[47]
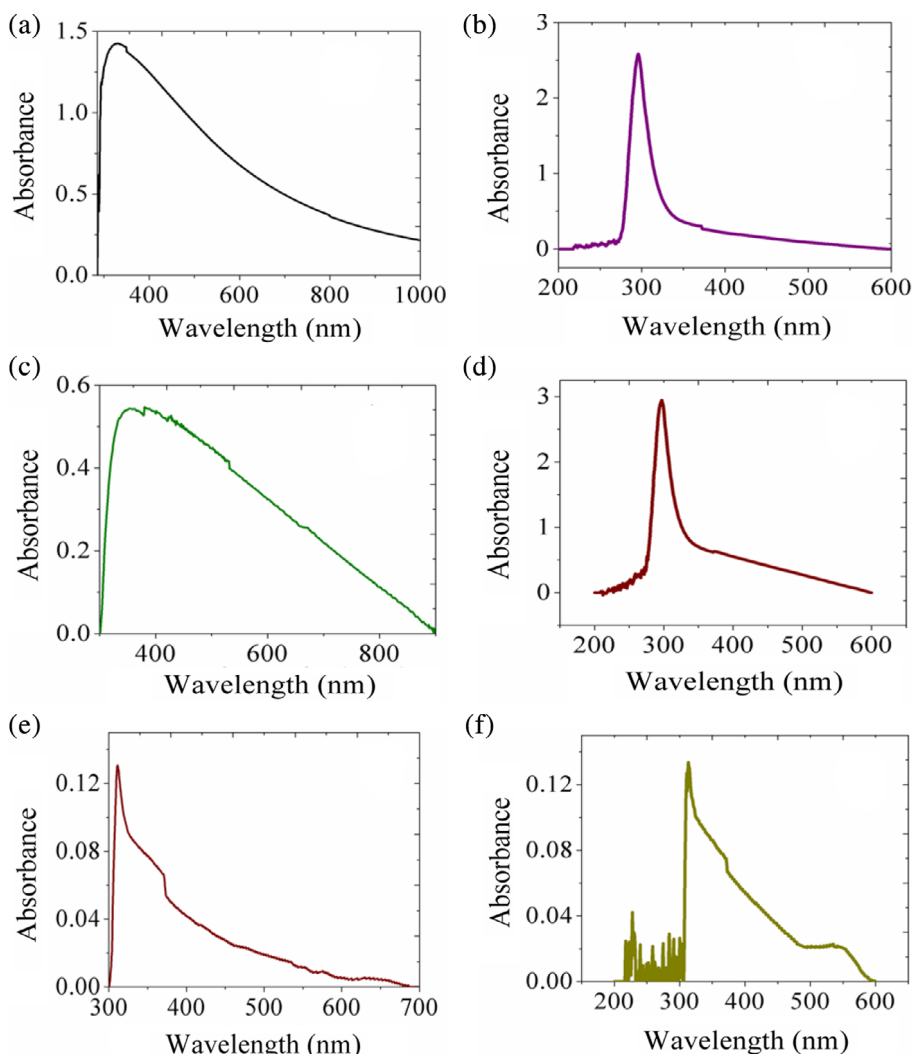

FIGURE 12 UV–visible analysis spectra: (a) pure PMMA nanofibers (b) pure PMMA nanofibers incorporated with gold nanoparticles (c) surface roughened PMMA nanofibers (d) surface roughened PMMA nanofibers incorporated with gold nanoparticles (e) coaxial hollow PMMA nanofibers (f) coaxial hollow PMMA nanofibers incorporated with gold nanoparticles [Color figure can be viewed at wileyonlinelibrary.com]

The increase in excitation wavelength also results in blue shift of the PL peaks due to the changes in luminescence transition of PMMA nanofibers and SPR. Hence, it can be concluded that PMMA nanofibers act as better host matrix to AuNPs with enhanced intensity.

Surface roughened PMMA nanofibers are also subjected to different excitation wavelengths and the maximum intensity observed at 340 nm, which is shown in Figure 13c. Surface roughened PMMA nanofibers incorporated with AuNPs are also subjected to different excitation wavelengths from 270 to 310 nm as shown in Figure 13d. Here, also it is observed that PMMA show a broad emission in 400–500 nm and the intensity of the PL peaks increases as excitation wavelength increases and the maximum intensity occurs at 310 nm with 600,000 cps. Here also the PL peaks show a blue shift with increase in excitation wavelength due to the influence of SPR of AuNPs. The peaks of AuNPs are obtained at 530–560 nm with a blue shift as the excitation wavelength increases. Surface roughened PMMA nanofibers

have maximum intensity 135,000 cps while it changes to 600,000 cps after incorporating AuNPs, which proves that surface roughened PMMA nanofibers can also act as better host matrix to noble metal nanoparticles like AuNPs.

Coaxial hollow PMMA nanofibers are showing maximum emission at 320 nm among the different excitation wavelengths as represented in Figure 13e. The PL spectrum of these nanofibers after incorporating with AuNPs is shown in Figure 13f. The AuNPs incorporated coaxial hollow PMMA nanofibers are also subjected to excitation wavelengths ranging from 290 to 330 nm as per the absorption maximum values from UV–Visible analyses. Here, also it is found that the intensity of emission increases with increase in excitation wavelength and maximum intensity occurs at 330 nm with 160,000 cps.

The PL peaks of PMMA nanofibers are observed at 400–450 nm as shown in Figure 13f while the AuNPs show peaks at 500–550 nm. The peaks of PMMA nanofibers found to suppress the emission peaks of AuNPs in this sample. The coaxial hollow PMMA
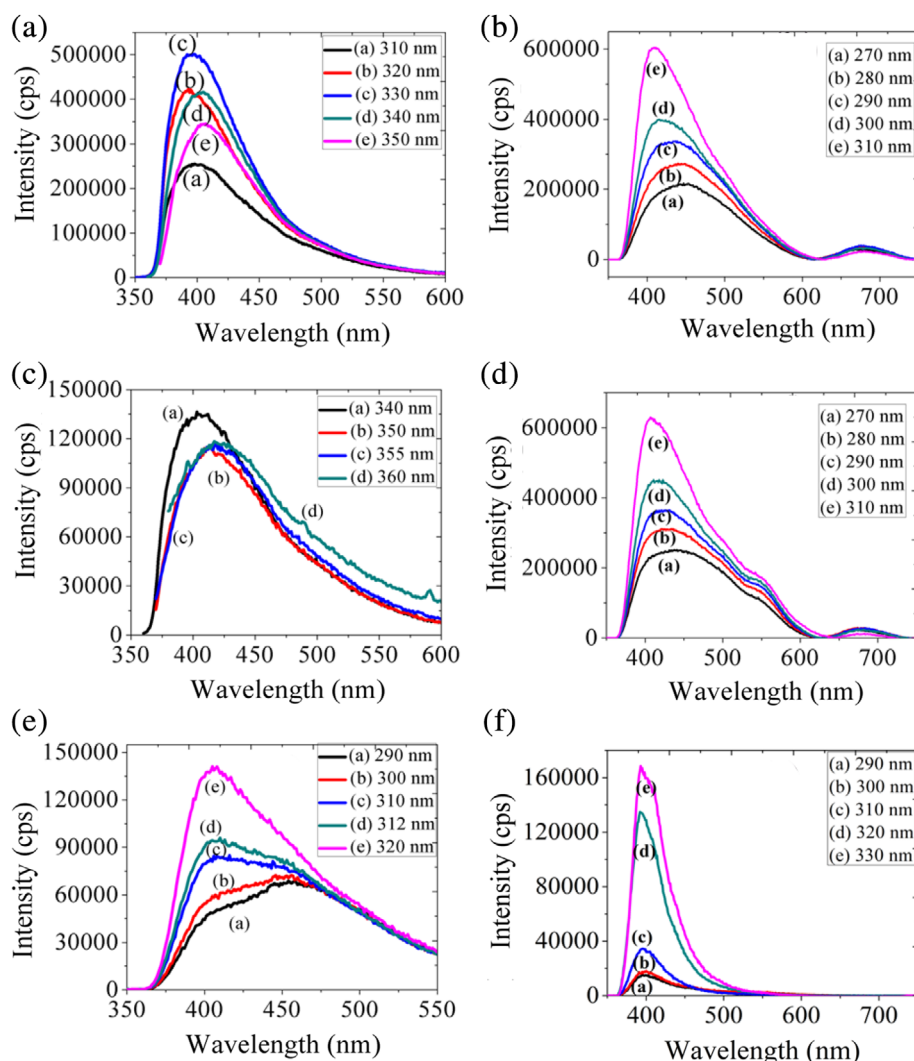

FIGURE 13 PL spectra: (a) pure PMMA nanofibers (b) pure PMMA nanofibers incorporated with gold nanoparticles (c) surface roughened PMMA nanofibers (d) surface roughened PMMA nanofibers incorporated with gold nanoparticles (e) coaxial hollow PMMA nanofibers (f) coaxial hollow PMMA nanofibers incorporated with gold nanoparticles [Color figure can be viewed at wileyonlinelibrary.com]

nanofibers found to have maximum intensity 150,000 cps whereas those incorporated with AuNPs show 160,000 cps. This enhancement in intensity is an evidence for the capacity of coaxial hollow PMMA nanofibers to act as host matrices for different nanoparticles like AuNPs. The PL results of the pure, surface roughened and coaxial hollow PMMA nanofibers and those incorporated with AuNPs are thus supports the other structural and molecular analyses.

5 | COMPARISON OF THE HOST MATRIX NATURE OF PURE AND STRUCTURALLY MODIFIED PMMA NANOFIBERS BY COMPARING THE OPTICAL PROPERTIES OF THE PURE AND STRUCTURALLY MODIFIED PMMA NANOFIBERS BEFORE AND AFTER INCORPORATING GOLD NANOPARTICLES

A comparative study is carried out between the pure and structurally modified PMMA nanofibers and those incorporated with gold nanoparticles to identify the host matrix nature of PMMA nanofibers to gold nanoparticles. Pure PMMA shows maximum intensity at almost 500,000 cps while that incorporated with gold nanoparticles show almost 600,000 cps. The surface roughened PMMA nanofibers show maximum intensity at 135,000 cps and that incorporated with gold nanoparticles show 600,000 cps. The coaxial hollow PMMA nanofibers show maximum intensity at 150000 cps and that incorporated with gold nanoparticles show 160,000 cps.

It is observed that, the pure and structurally modified PMMA nanofibers show an enhancement in intensity on incorporation with gold nanoparticles, which proves the host matrix nature of PMMA to gold nanoparticles. It is observed from the comparative studies among the pure and structurally modified PMMA nanofibers incorporated with AuNPs that the PL intensity enhancement is higher in the case of surface roughened PMMA nanofibers incorporated with AuNPs compared to that of the pure and coaxial hollow PMMA nanofibers. This is due to the more uniform distribution of AuNPs in it compared to the other two forms as supported by TEM analyses results shown in Figure 9. The voids, pits, depressions and other surface characteristics present in the surface of surface roughened PMMA nanofibers, which is absent in the pure and coaxial hollow structural

forms, make them suitable to act as better host matrix to AuNPs than the other two. Thus, it is proved from this study that the optical properties of these PMMA nanofibers also can be improved by incorporating luminescent nanoparticles like AuNPs, which broadens their applications. Host matrix nature of PMMA nanofibers can be further improved by modifying their surface as given here. The better host matrix nature of surface roughened PMMA nanofibers is thus evidenced by all the above-mentioned analyses.

6 | APPLICATIONS

PMMA nanofibers have many applications in optical fields due to their transparency, rigidity and stability compared to other polymeric systems. These characteristic properties of PMMA are combined with the SPR of AuNPs to make it more attractive and applicable. PMMA nanofibers incorporated with AuNPs found applications in many areas like in capacitors, light and flexible electronic devices, sensors,[8,48] catalysis[49] etc. The incorporation of these AuNPs to structurally modified electrospun PMMA nanofibers like surface roughened and coaxial hollow PMMA forms offer much more unique properties and advantages than the AuNPs incorporated pure PMMA nanofibers and this further raises their applications.

7 | CONCLUSION

The pure and structurally modified PMMA nanofibers are produced by tuning the electrospinning process and parameters. The surface properties and characteristics of the produced fibers are proved by different characterization techniques like FESEM, TEM and AFM. The pure and structurally modified PMMA nanofibers incorporated with AuNPs are produced by the dispersion method. The successful incorporation of the AuNPs to all the three forms of PMMA nanofibers are proved through FTIR, XRD, FESEM, TEM and EDX analyses. The photoluminescence analysis of the PMMA nanofibers show their emission in visible region, which is much enhanced after incorporating AuNPs to them. This is due to the influence of luminescence transitions and SPR of AuNPs on the transparent PMMA nanofibers. The transparency of PMMA nanofibers combines with the luminescence of AuNPs to make them more suitable in optical devices and other optical fields. The successful incorporation of AuNPs to the pure and structurally modified PMMA

nanofibers proves their host matrix nature for various nanomaterials. Comparison of the host matrix nature of pure, surface roughened and coaxial hollow PMMA nanofibers by comparing their optical enhancement after incorporating AuNPs show that the surface roughened PMMA nanofibers act as better host matrix than the pure and coaxial hollow PMMA nanofibers with uniform distribution of AuNPs. This superior property of surface roughened PMMA nanofibers can be used in all the fields of PMMA nanofibers like optical works, catalytically supporting agents, antibacterial supporting systems etc.

ACKNOWLEDGMENT

CONFLICT OF INTEREST

The authors declare no conflict of interest.

ORCID

Tomlal Jose [ORCID] https://orcid.org/0000-0002-5390-7621

REFERENCES

[1] Z. M. Huang, Y. Z. Zhang, M. Kotaki, S. Ramakrishna, *Compos. Sci. Technol.* **2003**, *63*, 2223.

[2] D. A. Gopakumar, V. Arumukhan, R. V. Gelamo, D. Pasquini, L. C. Morais, S. Rizal, D. Hermawan, A. Nzihou, H. P. S. A. Khalil, *Nano-Struct. Nano-Obj.* **2019**, *18*, 100268.

[3] A. Frenot, I. S. Chronakis, *Curr. Opin. Colloid Interface Sci.* **2003**, *8*, 64.

[4] N. Bhardwaj, S. C. Kundu, *Biotechnol. Adv.* **2010**, *28*, 325.

[5] R. Vijayan, S. Joseph, B. Mathew, *Bioprocess. Biosyst. Eng.* **2018**, *42*(2019), 305.

[6] V. R. Raja, D. R. Rosaline, A. Suganthi, M. Rajarajan, *Solid State Sci.* **2017**, *67*, 99.

[7] A. V. Borhade, B. K. Uphade, *Chalcogenide Lett.* **2012**, *9*, 299.

[8] I. Capek, *Encycl. Life Support Syst.* **2020**, *115*, 1.

[9] K. Ghosal, A. Chandra, G. Praveen, S. Snigdha, S. Roy, C. Agatemor, S. Thomas, I. Provaznik, *Sci. Rep.* **2018**, *8*, 1.

[10] Y. Li, B. Yin, T. Wang, J. Zhou, J. Wang, W. Luo, R. Tang, Z. Cao, N. Yuan, X. Du Li, C. Wang, S. Zhao, Y. Liu, Z. L. Wang, *ACS Nano* **2017**, *11*, 10439.

[11] Y. Han, J. Zou, Z. Li, W. Wang, Y. Jie, J. Ma, B. Tang, Q. Zhang, X. Cao, S. Xu, Z. L. Wang, *ACS Nano* **2018**, *12*, 4835.

[12] K. Bicy, S. Suriyakumar, P. Anu Paul, A. S. Anu, N. Kalarikkal, A. M. Stephen, V. G. Geethamma, D. Rouxel, S. Thomas, *New J. Chem.* **2018**, *42*, 19505.

[13] R. Arumugam, E. S. Srinadhu, B. Subramanian, S. Nallani, *Med. Hypotheses* **2019**, *122*, 31.

[14] A. Haider, S. Haider, I. K. Kang, *Arab. J. Chem.* **2018**, *11*, 1165.

[15] S. Thenmozhi, N. Dharmaraj, K. Kadirvelu, H. Y. Kim, *Mat. Sci. Eng. B* **2017**, *217*, 36.

[16] P. Raghavan, D. H. Lim, J. H. Ahn, C. Nah, D. C. Sherrington, H. S. Ryu, H. J. Ahn, *React. Funct. Polym.* **2012**, *72*, 915.

[17] T. Uyar, E. Kny, *Electrospun Materials for Tissue Engineering and Biomedical Applications*, Woodhead Publishing, UK **2017**, p. 1.

[18] B. Ding, J. Yu, *Electrospun Nanofibers for Energy and Environmental Applications*, Springer, Verlag Berlin Heidelberg **2014**, p. 355.

[19] R. Augustine, H. N. Malik, D. K. Singhal, A. Mukherjee, D. Malakar, N. Kalarikkal, S. Thomas, *J. Polym. Res.* **2014**, *21*, 347.

[20] P. Harikrishnan, A. Sivasamy, *Nano-Struct. Nano-Obj.* **2020**, *23*, 100518.

[21] J. B. Branco, A. C. Ferreira, T. A. Gasche, J. P. Leal, *Nano-Struct. Nano-Obj.* **2018**, *15*, 75.

[22] K. Aruchamy, A. Mahto, S. K. Nataraj, *Nano-Struct. Nano-Obj.* **2018**, *16*, 45.

[23] V. P. Dinesh, R. Sriram kumar, A. Sukhananazerin, J. Mary Sneha, P. Manoj Kumar, P. Biji, *Nano-Struct. Nano-Obj.* **2019**, *19*, 100311.

[24] H. Dong, K. E. Strawhecker, J. F. Snyder, J. A. Orlicki, R. S. Reiner, A. W. Rudie, *Carbohydr. Polym.* **2012**, *87*, 2488.

[25] T. P. Lodge, E. R. Wood, J. C. Haley, *J. Polym. Sci. A* **2006**, *44*, 756.

[26] H. Abdali, A. Ajji, *Polymers* **2017**, *9*, 453.

[27] L. Zhou, N. Wu, Q. Cao, B. Jing, X. Wang, Q. Wang, H. Kuang, *Solid State Ion* **2013**, *249–250*, 93.

[28] S. L. Quan, H. S. Lee, E. H. Lee, K. D. Park, S. G. Lee, I. J. Chin, *Microelectron. Eng.* **2010**, *87*, 1308.

[29] H. C. Kim, B. G. Choi, J. Noh, K. G. Song, S. H. Lee, S. K. Maeng, *Desalination* **2014**, *346*, 107.

[30] H. D. Zhang, C. C. Tang, Y. Z. Long, J. C. Zhang, R. Huang, J. J. Li, C. Z. Gu, *Sens. Actuators A* **2014**, *219*, 123.

[31] X. Y. Sun, L. R. Nobles, H. G. Borner, R. J. Spontak, *Macromol. Rapid Commun.* **2008**, *29*, 1455.

[32] P. Philip, P. Thomas, T. Jose, K. C. Philip, P. C. Thomas, *Bull. Mater. Sci.* **2019**, *42*, 218.

[33] M. K. Abyaneh, S. Jafarkhani, S. K. Kulkarni, *J. Exp. Nanosci.* **2011**, *6*, 159.

[34] A. Sreekumaran Nair, R. T. Tom, V. R. Rajeev Kumar, C. Subramaniam, T. Pradeep, *COSMOS* **2007**, *3*, 103.

[35] M. Alsawafta, S. Badilescu, A. Paneri, V. V. Truong, M. Packirisamy, *Polymers* **2011**, *3*, 1833.

[36] L. A. Dykman, V. A. Bogatyrev, *Russ. Chem. Rev.* **2007**, *76*, 181.

[37] Y. S. Seo, E. Y. Ahn, J. Park, T. Y. Kim, J. E. Hong, K. Kim, Y. Park, Y. Park, *Nanoscale Res. Lett.* **2017**, *12*, 7.

[38] S. S. R. Gupta, M. L. Kantam, B. M. Bhanage, *Nano-Structures and Nano-Objects* **2018**, *14*, 125.

[39] C. S. Rejiya, J. Kumar, V. Raji, M. Vibin, A. Abraham, *Pharmacol. Res.* **2012**, *65*, 261.

[40] Y. Z. Li, Z. H. Huang, Y. Q. Yang, W. K. Zhang, L. Z. Gao, W. J. Chen, *Inorg. Nano-Metal Chem.* **2017**, *47*, 244.

[41] D. Basak, S. Karan, B. Mallik, *Chem. Phys. Lett.* **2006**, *420*, 115.

[42] P. Philip, T. Jose, J. K. Chacko, K. C. Philip, P. C. Thomas, *Polym. Test* **2019**, *74*, 257.

[43] S. Joseph, B. Mathew, *Spectrochim. Acta A* **2015**, *136*, 1371.

[44] S. N. Sawant, V. Selvaraj, V. Prabhawathi, M. Doble, *PLoS One* **2013**, *8*(5), e63311.

[45] G. A. Kaur, M. Shandilya, P. Rana, S. Thakur, P. Uniyal, *Nano-Struct. Nano-Obj.* **2020**, *22*, 100428.

[46] D. He, B. Hu, Q. F. Yao, K. Wang, S. H. Yu, *ACS Nano* **2009**, *3*, 3993.

[47] P. Philip, T. Jose, K. C. Philip, P. Manoj, T. Sajini, *Mater. Today Proc.* **2020**. https://doi.org/10.1016/j.matpr.2020.03.681.

[48] J. Gao, J. Fu, C. Lin, J. Lin, Y. Han, X. Yu, C. Pan, *Langmuir* **2004**, *20*, 9775.

[49] S. D. Solomon, M. Bahadory, A. V. Jeyarajasingam, S. A. Rutkowsky, C. Boritz, *J. Chem. Educ.* **2007**, *84*, 322.